# Measuring the Three-Dimensional Structure of Ultrathin Insulating Films at the Atomic Scale

**Susanne Baumann,[†,‡] Ileana G. Rau,[†] Sebastian Loth,[§,⊥] Christopher P. Lutz,[†] and Andreas J. Heinrich[†,*]**

[†]IBM Almaden Research Center, 650 Harry Road, San Jose, California 95120, United States, [‡]Department of Physics, University of Basel, Klingelbergstrasse 82, 4056 Basel, Switzerland, [§]Max Planck Institute for the Structure and Dynamics of Matter, 22761 Hamburg, Germany, and [⊥]Max Planck Institute for Solid State Research, 70569 Stuttgart, Germany

**ABSTRACT** The increasing technological importance of thin insulating layers calls for a thorough understanding of their structure. Here we apply scanning probe methods to investigate the structure of ultrathin magnesium oxide (MgO) which is the insulating material of choice in spintronic applications. A combination of force and current measurements gives high spatial resolution maps of the local three-dimensional insulator structure. When force measurements are not available, a lower spatial resolution can be obtained from tunneling images at different voltages. These broadly applicable techniques reveal a previously unknown complexity in the structure of MgO on Ag(001), such as steps in the insulator–metal interface.

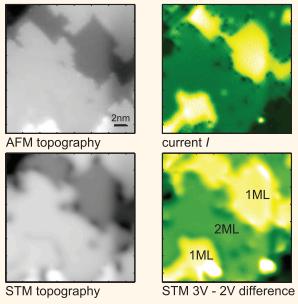


**KEYWORDS:** magnesium oxide · atomic force microscopy · conductive AFM · scanning tunneling microscopy · thickness determination · thin oxide films · thin insulating films

Ultrathin insulating films provide precise electrostatic coupling and electron tunneling from a conducting substrate to a second electrode or to adsorbed nanostructures.[1] Such films have long served as gate insulators and tunnel junctions,[2] and they are gaining use as tunable catalytic surfaces[3] and substrates for magnetic nanostructures.[4] Magnesium oxide (MgO) films in particular are increasingly used in these roles[5–9] and can be grown epitaxially with monolayer thickness control. The precise film thickness and structure determines the coupling, so techniques to characterize the films at the atomic scale are essential.

Here we show how scanning probe methods can be used not only to determine the exact local film thickness of a thin insulator but also to resolve its three-dimensional structure. We use scanning tunneling microscopy (STM) and conductive atomic force microscopy (AFM), which is a combination of STM and standard AFM,[10–12] to measure the richly varied structure of thin MgO films grown on Ag(001) and to determine the MgO thickness as well as the topography of the buried MgO–Ag interface. In conductive AFM, we record the tunnel current while scanning the tip with constant force interaction over the surface (Figure 1a). This allows us to characterize the full three-dimensional structure of the thin insulator with atomic resolution and reveals the rather complex morphology of MgO on Ag. On the basis of our conductive AFM measurements, we demonstrate a method to determine the structure of the thin insulating film solely based on STM by making use of the electronic properties of MgO films. We show that the latter approach is only feasible in high-quality thin films and results in a lateral resolution of about 2 nm. The two techniques for thickness determination can be adapted in a straightforward way to thin films of other insulating materials on conducting substrates.

Aspects of the structure of different ultrathin films, including MgO, have previously been studied with various scanning probe techniques. In particular, electronic properties of thin MgO films on various metal substrates have been investigated with STM.[13–15] These properties were then applied to determine some aspects of the MgO thickness.[16,17] Atomic-scale spatial resolution with AFM has been demonstrated

* Address correspondence to andreash@us.ibm.com.

Received for review November 27, 2013 and accepted December 30, 2013.

**Published online December 30, 2013**
**10.1021/nn4061034**

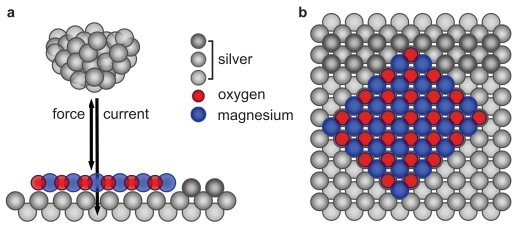


**Figure 1. Combined STM and AFM setup. (a) STM tip is mounted on an AFM cantilever to allow simultaneous measurements of the force between the tip and the surface of the insulating film and the current to the underlying Ag substrate. (b) Top view of the MgO film on Ag(001). Oxygen atoms are on top of the Ag atoms and the magnesium atoms in the hollow sites.[25] MgO preferably forms edges along the nonpolar direction, with alternating oxygen and magnesium atoms along the edge.**

on cleaved MgO(001) single crystals and MgO thin films.[18,19] The combined use of AFM and STM on MgO has been used to distinguish between different kinds of defects[20] and to determine work function shifts.[21] Here we use the combination of scanning probe techniques to determine the three-dimensional structure of the MgO films and to image the topography of the MgO/Ag interface. Conductive AFM on large areas has been used as a method for the thickness determination on a different material, aluminum oxide on Co, but lacked lateral atomic resolution.[22] Electronic contrasts in STM were used on nickel oxide on Ag to determine the insulator thicknesses locally.[23] Here we show that on MgO a careful thickness determination of the thin insulating films with conductive AFM is needed to properly interpret the varied bias-dependent contrasts observed in STM.

## RESULTS AND DISCUSSION

The thin films of MgO on Ag(001) were grown in a room temperature vacuum chamber and transferred in vacuum to the cold scanning probe microscope (see Methods for details). All experiments were performed with a home-built STM/AFM operating at low temperature (6 K) and in ultrahigh vacuum. The microscope has a force sensor with a conductive probe tip.[24] The simultaneous recording of force and tunneling current (Figure 1a) allows the characterization of MgO films with atomic-scale lateral as well as vertical thickness resolution. The force channel maps the topography of the surface and is used to regulate the tip−sample distance, while at the same time, the tunnel current channel maps the thickness of the MgO layer.

In AFM operation, we detect the frequency shift (FM-AFM) of the cantilever due to the tip's interaction with the surface.[26] The cantilever operates at small constant oscillation amplitude (~0.1 nm peak-to-peak) and is sensitive primarily to the force gradient of the atomic-scale junction, rather than to background forces between the larger-scale tip and the surface.[27]

An AFM image of a typical MgO sample recorded at a constant frequency shift of $\Delta f = -25$ Hz is shown

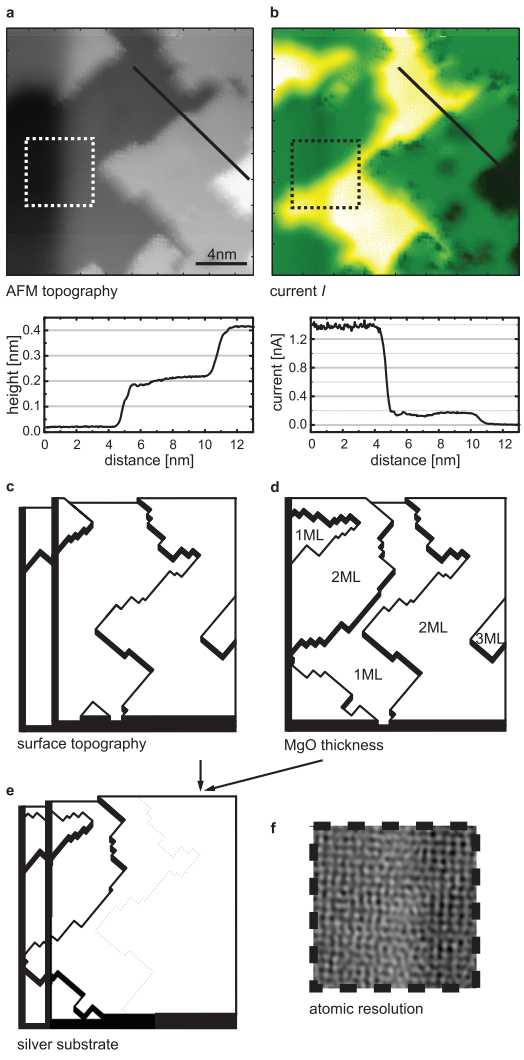


**Figure 2. Comparison of AFM and tunnel current measurements over several MgO layers. (a) AFM topography of ~2 ML MgO grown on Ag(001) ($\Delta f = -25$ Hz, $V = -5$ mV, 20 × 20 nm$^2$). (b) Simultaneously with the AFM topography, the tunnel current is recorded. Changes in the current are due to changes in the thickness of the MgO barrier between the tip and the Ag substrate. The tunnel current image (b) differs significantly from the topography (a), which indicates different local MgO thickness and subsurface Ag steps. This complex sample structure is schematically shown in (c−e). (c) Topography of the top surface of the MgO (schematic drawing of (a)). (d) Thickness of the MgO (without the Ag substrate), which is indicated directly by the current image in (b). (e) Schematic drawing of the underlying Ag topography inferred from (a) and (b) (see text). (The dotted line indicates a MgO thickness change associated with a surface step.) (f) Atomic resolution in an enlarged view of (a) (area indicated in (a,b), 5.6 × 5.6 nm$^2$). The atomic resolution continues over one and two monolayers of MgO, as well as over an underlying Ag step which is not accompanied by a change in the MgO thickness.**

in Figure 2a. This frequency shift corresponds to an attractive interaction with a force gradient of 4 N/m (see Methods), which is about a tenth of the stiffness of a single chemical bond (10−100 N/m). Subject to such strong force interaction, the tip is near mechanical contact with the surface, and the AFM image reveals

the surface topography of the MgO film on Ag(001). We observe ~5 nm wide terraces with a step height of 0.20 ± 0.01 nm between neighboring terraces. This step height agrees well with the bulk MgO atomic layer thickness of 0.21 nm.[28]

While acquiring this AFM image, a small surface-to-tip bias voltage was applied ($V = -5$ mV) and the tunnel current ($I$) was recorded (Figure 2b). At this low bias, the MgO has no electronic states accessible to tunneling electrons. It acts as an insulating tunneling barrier similar to the vacuum tunnel junction albeit with different barrier height. The tunnel current image (Figure 2b) is remarkably different from the AFM topographic image (Figure 2a): changes in the current often do not coincide with steps in the AFM topograph. In tunnel junctions, the tunnel current is exponentially sensitive to the width of the barrier between the tip and the conducting substrate. Differences in this current thus provide a sensitive measure of the insulating film thickness—the thicker the film, the smaller the tunnel current. We find that the tunnel current decreases by a factor of ~8 for each additional monolayer of MgO. The comparison of Figure 2a,b shows that MgO changes its thickness not only at steps related to the surface topography but also at locations where the surface is smooth, which indicates that there must be additional steps in the underlying substrate. The schematic drawings in Figure 2 illustrate the resulting three-dimensional structure of the thin MgO film by independently showing the topography of the surface−vacuum interface (c), the MgO thickness (d), and the topography of the underlying Ag substrate (e) of the same area.

Magnesium oxide on Ag(001) grows with the oxygen atoms on top of the Ag atoms and the magnesium atoms in the hollow sites (Figure 1a).[25,29,30] Individual atomic layers of MgO are known to terminate preferably along nonpolar edges, in which oxygen and magnesium atoms are alternating along the edge (Figure 1b).[29,30] Figure 2b shows that most changes of the MgO thickness occur by forming such nonpolar edges (45° to the image axes in the figure). Nonpolar MgO edges occur both atop the MgO film and at the buried MgO/Ag interface, where a matching Ag step occurs in order to preserve the crystalline order. In addition to the nonpolar MgO edges, the underlying Ag substrate in Figure 2 also shows a step parallel to a polar MgO direction (vertical feature along left edge in Figure 2a,e). However, Figure 2b shows that the thickness of the MgO film does not change along that Ag edge. A magnified view of the AFM topography above part of this feature (Figure 2f) reveals that MgO layers avoid forming what would be a polar step edge, by using a carpet-like growth mode, in which the film is draped smoothly over the Ag step without introducing any edges in the MgO layers.[31,32] This carpet-like growth appears in both single- and double-layered MgO regions of this figure.

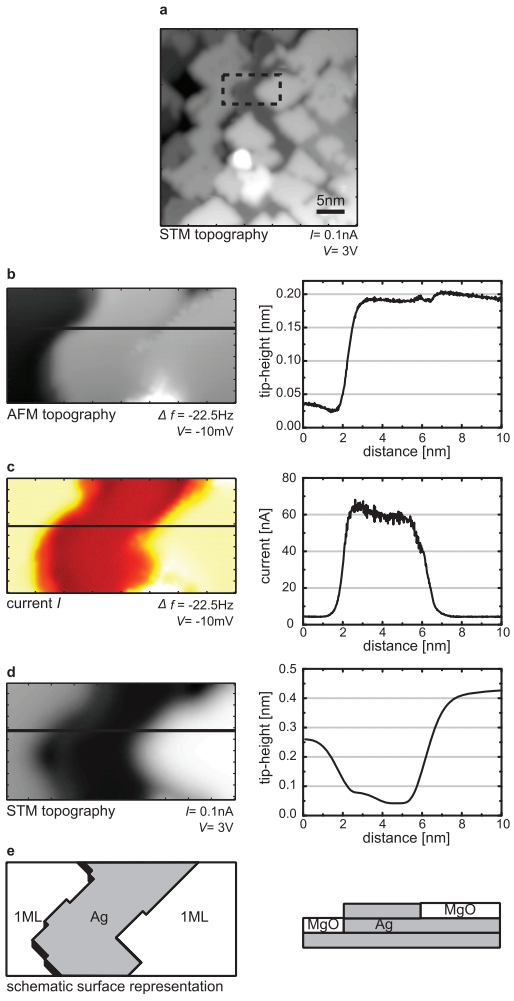


**Figure 3. Embedded MgO islands on Ag(001). (a) STM topography shows single monolayer MgO islands ($I$ = 0.1 nA, $V$ = 3 V, 35 × 35 nm$^2$). (b) AFM topography (constant $\Delta f$ = −22.5 Hz, so tip is near contact with the surface) shows MgO islands embedded in the Ag substrate. The top surface of the MgO is coplanar with the Ag region (right side of the image, 5 × 10 nm$^2$) or recessed by one monolayer (left). (c) Tunnel current image obtained simultaneously with the AFM topography ($V$ = −10 mV) distinguishes regions covered by one monolayer of MgO from bare Ag regions. (d) Constant-current STM topography of the same area recorded at high bias in order to tunnel into the surface state of the MgO ($I$ = 0.1 nA, $V$ = 3 V). (e) Schematic cross section of the surface. Comparison between the two topographies (b,d) indicates an apparent height of 0.6 nm for the first monolayer of MgO in STM imaging at 3 V.**

Repeated cycles of sputtering and annealing of the silver crystal leave a flat Ag surface with atomically flat terraces of ~100 nm width as verified by STM imaging before MgO film deposition. We therefore conclude that most of the observed steps at the MgO/Ag interface arise during the epitaxial growth of the MgO, which is consistent with the occurrence of mostly nonpolar step edges. For submonolayer MgO, an AFM image and its corresponding tunneling current image are shown in Figure 3b,c. The AFM topography (Figure 3b) and simultaneously acquired tunnel current (Figure 3c) show single monolayer MgO islands

embedded into the Ag substrate. The AFM image shows the two most frequently observed cases: the top surface of the MgO lies in essentially the same plane as the adjacent region of bare Ag(001) (right side of figure), or it lies one monolayer below (left side). The current image (Figure 3c) recorded simultaneously with the AFM topography ($V = -10$ mV) shows clear differences between the MgO islands and the bare Ag substrate. The current decreases by a factor of ~13 when moving the tip from the metal to the first monolayer of MgO. Samples prepared with submonolayer MgO coverage predominantly show areas having only one monolayer of MgO. It therefore appears that MgO starts growing in single layers unlike NaCl, which often occurs in double layers first.[33] The conductance measured on these one monolayer MgO islands closely matches that observed for the lowest MgO thickness seen in the ~2 ML sample of Figure 2b, which corroborates the assignment of 1 ML to those regions. The observed embedded islands indicate that the MgO prefers to terminate its edges at a matching Ag step rather than at the vacuum interface. Such embedded structures have been predicted to be energetically favorable over islands on top of the Ag substrate.[30]

These conductive AFM results reveal a surprising variety in the morphology of MgO films on Ag(001), in which embedded islands are intermixed with on-top islands and carpet-like coverage of some Ag steps. Some of these observed features, such as embedded islands for submonolayer coverage, have been observed previously.[14,16] Here we show how thicker oxide films of MgO also form islands at the MgO/Ag interface, where they terminate at matching Ag steps, rather than forming a continuous first monolayer.

Scanning tunneling microscopy can be used to further investigate the electronic properties of the MgO films. In particular, electronic states close to the surface can be identified with tunneling spectroscopy. The bare Ag substrate shows a flat d$z$/d$V$ spectrum between 0.5 and 4 V (not shown), while the MgO film shows two prominent d$z$/d$V$ peaks (Figure 4). These peaks have been previously identified as corresponding to the interface state between the Ag(001) and the MgO at ~2 V and a MgO surface state (or its conduction band edge) at ~2.5 V.[14,29,34,35] Figure 4a shows a continuous line of d$z$/d$V$ spectra, sweeping the tip laterally over 1−4 monolayers of MgO (Figure 4b,c). This spectral map shows the evolution of the electronic states as the tip passes over a variety of surface features: the MgO/Ag interface state remains roughly constant in magnitude, while the MgO state shows a strong dependence on the film thickness. (For a comparison between d$z$/d$V$ and previous thickness-dependent spectroscopic STM methods,[14] see Supporting Information.)

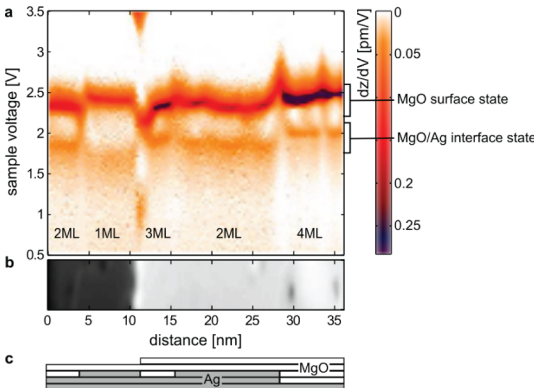


**Figure 4. d$z$/d$V$ spectroscopy over MgO of different thickness. Numerical derivative d$z$/d$V$ of $z(V)$ spectra in constant-current mode ($I$ = 10 pA). (a) Sequence of d$z$/d$V$ spectra recorded along a line across the surface. The d$z$/d$V$ signal is plotted color-coded as a function of lateral position and voltage (white, low signal; dark, high signal). MgO has two characteristic states: an interface state at ~2 V (state at the interface between the Ag and MgO) and a surface state at ~2.5 V.[14] The line of spectra in (a) extends over 1−4 monolayers of magnesium oxide, with changes on the surface as well as in the underlying interface (b,c). (b) STM topograph ($V$ = 3 V, $I$ = 10 pA) shows the top surface of the MgO. (c) Schematic drawing of the same area. The MgO states are perturbed for several nanometers around locations where the MgO thickness changes.**

A bias of 3 V or more is commonly used in STM images of MgO thin films.[13,14] This voltage is well above the d$z$/d$V$ peak associated with the MgO state, so tunneling into the surface of the MgO is allowed. Thus these images resemble the surface topography of the MgO (see Figure 5a, compared to Figure 2a). However, when the bias voltage is below the characteristic MgO state (*e.g.*, 2 V), the electrons can only tunnel into the interface state or into the Ag substrate directly (Figure 5b), which gives a distinctly different image.[13,16,17] The 2 V image contains information about the topography of the metal surface below the thin insulating layer, modulated by the thickness of the film. In Figure 5c, we show the difference of those two scanning voltages, which can be understood as the difference between scanning the top of the MgO and scanning the interface between the oxide and the metal substrate, and thus the "bottom" of the MgO. Such a difference image therefore reveals the thickness of the MgO. Indeed, the STM difference image (Figure 5c) shows the same MgO thickness map as the conductive AFM image (Figure 2b), albeit with reduced spatial resolution. At these voltages, the difference between individual MgO layers appears as a height change of ~0.1 nm (Figure 5d).

These measurements show that thickness determination can be carried out by a STM-only method on scanning probe systems without AFM capability. However, when using STM on a submonolayer coverage of

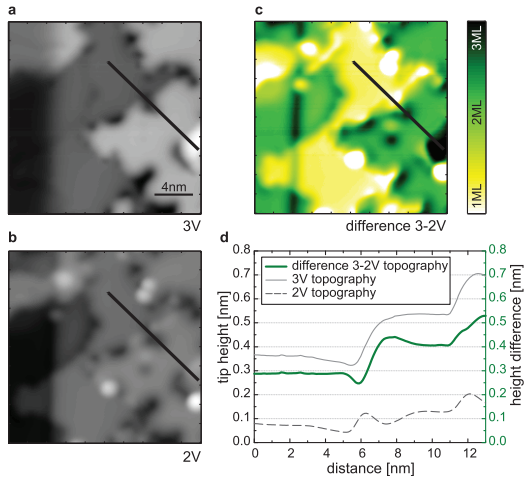


**Figure 5. MgO thickness determination with STM. Measurements of the same area as in Figure 2 on ~2 ML MgO/Ag(001). (a) STM image at 3 V, where electrons are tunneling into the surface state (compare to Figure 2a,c), and (b) at 2 V, which corresponds to tunneling into the MgO−Ag interface or the Ag substrate (Figure 2e). (c) Difference between the 3 and 2 V images, which is comparable to Figure 2b,d. This difference is therefore an alternative way to determine the thickness of the MgO. (d) Line cuts of all three images. $I = 0.1$ nA in all images, 20 × 20 nm$^2$.**

MgO, care should be taken with the STM-only technique since embedded islands, as shown in Figure 3, appear as tall protrusions with respect to the Ag substrate. For example, the MgO island that appears 0.2 nm lower than the Ag substrate in the AFM channel (Figure 3a) appears as a 0.2 nm protrusion in STM imaging (Figure 3d). This thus carries the risk of assigning these apparent 0.2 nm protrusions as MgO islands grown atop the Ag substrate.[16,17] Here we use the AFM channel to unambiguously show that these islands are embedded into the Ag surface.

By comparing the STM and AFM measurements, we can draw two important conclusions. First, as long as the surface is covered with more than a full monolayer of MgO, we find that STM imaging at ~3 V gives an accurate representation of the surface topography (compare the AFM image of Figure 2a with the STM image of Figure 5a). However, for submonolayer coverage of MgO, where some bare Ag regions are exposed, these STM images at high bias do not represent the surface topography as revealed by AFM (Figure 3). The large apparent height in STM (Figure 3d) of the first monolayer is presumably due to the reduced barrier energy (work function) above MgO compared to bare Ag.

Second, Figure 4a shows that the MgO state and the MgO/Ag interface state are clearly resolved only ~2 nm laterally away from any step edges. This is true for both surface and buried MgO steps. This wide border area of the MgO island's electronic structure also becomes visible by comparing the AFM and STM images, where the steps in the STM topography do not appear as sharp edges. Thickness determination with STM-only measurements thus yields an effective spatial resolution of 2 nm and requires samples with sufficiently large insulator terraces.

## CONCLUSIONS

The present paper demonstrates measurement of the thickness of a thin insulating film on a metal substrate with high spatial resolution scanning probe methods. Simultaneous AFM and STM measurements are used to give a clear picture of the complex three-dimensional structure of thin magnesium oxide films on Ag(001). We find that thickness changes can occur independently from surface steps revealing embedded islands and carpet-like growth of MgO films. The techniques presented here for the three-dimensional thickness determination should be applicable to other thin insulating films and should thus open new possibilities for thickness-dependent studies such as tuning the decoupling of individual atoms or molecules from their metal substrate or for studying thickness-dependent catalytic reactions on the surface of thin insulators.

## METHODS

**Sample Preparation.** The protocol for growing MgO films on Ag(001) is similar to that used in earlier publications.[14,16,35] The Ag surface was cleaned by repeated cycles of sputtering ($Ar^+$, $p_{Ar} = 2 \times 10^{-6}$ Torr, 1 keV, 6 min) followed by annealing (680 K, 5 min) to obtain a clean Ag surface. After these cleaning cycles, the impurities were below the detection limit of an Auger electron spectrometer and STM images revealed a clean Ag substrate.

MgO thin films were epitaxially grown on the clean Ag(001) crystal by evaporating Mg onto the ~480 K surface, while exposing the surface to molecular oxygen gas ($p_{O_2} = 1 \times 10^{-6}$ Torr). The magnesium evaporation source was a homemade Knudsen cell kept at ~620 K and mounted 15 cm from the Ag surface to achieve a growth rate of ~1 ML per minute. The film preparation was done in the room temperature vacuum chamber, and the sample was passed through ultrahigh vacuum to the cold STM/AFM directly after the growth.

**AFM/STM.** The AFM measurements were done using an AFM with the qPlus sensor design having a resonance frequency of $f_0$ = 21 860 Hz and a spring constant $k_0$ of ~1800 N m$^{-1}$.[24] Oscillation amplitude was ~0.1 nm peak-to-peak. The force gradient is well approximated by $k = 2 \times k_0 \times (\Delta f/f_0)$.[27] A metal STM tip made of Ir, likely coated with Ag from the sample, was mounted on the AFM cantilever to allow simultaneous measurements of the current and force gradient.

**dz/dV Measurements.** For the d$z$/d$V$ measurements, the tip height ($z$) is recorded while voltage sweeps at constant current (closed feedback loop) are performed and subsequently the numerical derivative of the $z(V)$ curve is calculated. For Figure 4a, the tip was moved laterally by 0.1 nm between each recorded $z(V)$ spectrum. The observed peaks, or states, obtained with d$z$/d$V$ are systematically shifted with respect to some literature values[14] due to the specific spectroscopy method applied (see Supporting Information).

*Conflict of Interest:* The authors declare no competing financial interest.

*Acknowledgment.* The authors thank Bruce Melior for expert technical assistance. C.P.L. and A.J.H. thank the Office of Naval Research for financial support (N00014-11-C-0483).

*Supporting Information Available:* Comparison between thickness-dependent spectroscopic methods, along with another example of a conductive AFM to STM comparison. This material is available free of charge *via* the Internet at http://pubs.acs.org.

## REFERENCES AND NOTES


1. Repp, J.; Meyer, G.; Stojković, S. M.; Gourdon, A.; Joachim, C. Molecules on Insulating Films: Scanning-Tunneling Microscopy Imaging of Individual Molecular Orbitals. *Phys. Rev. Lett.* **2005**, *94*, 026803.
2. Sun, J.; Ralph, D. Magnetoresistance and Spin-Transfer Torque in Magnetic Tunnel Junctions. *J. Magn. Magn. Mater.* **2008**, *320*, 1227–1237.
3. Freund, H.-J.; Pacchioni, G. Oxide Ultra-thin Films on Metals: New Materials for the Design of Supported Metal Catalysts. *Chem. Soc. Rev.* **2008**, *37*, 2224–2242.
4. Loth, S.; Baumann, S.; Lutz, C. P.; Eigler, D. M.; Heinrich, A. J. Bistability in Atomic-Scale Antiferromagnets. *Science* **2012**, *335*, 196–199.
5. Parkin, S. S. P.; Kaiser, C.; Panchula, A.; Rice, P. M.; Hughes, B.; Samant, M.; Yang, S.-H. Giant Tunnelling Magnetoresistance at Room Temperature with MgO(100) Tunnel Barriers. *Nat. Mater.* **2004**, *3*, 862–867.
6. Yuasa, S.; Nagahama, T.; Fukushima, A.; Suzuki, Y.; Ando, K. Giant Room-Temperature Magnetoresistance in Single-Crystal Fe/MgO/Fe Magnetic Tunnel Junctions. *Nat. Mater.* **2004**, *3*, 868–871.
7. Yoon, B.; Häkkinen, H.; Landman, U.; Wörz, A. S.; Antonietti, J.-M.; Abbet, S.; Judai, K.; Heiz, U. Charging Effects on Bonding and Catalyzed Oxidation of CO on $Au_8$ Clusters on MgO. *Science* **2005**, *307*, 403–407.
8. Harding, C.; Habibpour, V.; Kunz, S.; Farnbacher, A. N.-S.; Heiz, U.; Yoon, B.; Landman, U. Control and Manipulation of Gold Nanocatalysis: Effects of Metal Oxide Support Thickness and Composition. *J. Am. Chem. Soc.* **2009**, *131*, 538–548.
9. Shin, H.-J.; Jung, J.; Motobayashi, K.; Yanagisawa, S.; Morikawa, Y.; Kim, Y.; Kawai, M. State-Selective Dissociation of a Single Water Molecule on an Ultrathin MgO Film. *Nat. Mater.* **2010**, *9*, 442–447.
10. Sawada, D.; Sugimoto, Y.; Morita, K.; Abe, M.; Morita, S. Simultaneous Measurement of Force and Funneling Current at Room Temperature. *Appl. Phys. Lett.* **2009**, *94*, 173117.
11. Polesel-Maris, J.; Lubin, C.; Thoyer, F.; Cousty, J. Combined Dynamic Scanning Tunneling Microscopy and Frequency Modulation Atomic Force Microscopy Investigations on Polythiophene Chains on Graphite with a Tuning Fork Sensor. *J. Appl. Phys.* **2011**, *109*, 074320.
12. Majzik, Z.; Drevniok, B.; Kamiński, W.; Ondráček, M.; McLean, A. B.; Jelínek, P. Room Temperature Discrimination of Adsorbed Molecules and Attachment Sites on the Si(111)-7 × 7 Surface Using a qPlus Sensor. *ACS Nano* **2013**, *7*, 2686–2692.
13. Gallagher, M.; Fyfield, M.; Cowin, J.; Joyce, S. Imaging Insulating Oxides: Scanning Tunneling Microscopy of Ultrathin MgO Films on Mo(001). *Surf. Sci.* **1995**, *339*, L909–L913.
14. Schintke, S.; Messerli, S.; Pivetta, M.; Patthey, F.; Libioulle, L.; Stengel, M.; De Vita, A.; Schneider, W.-D. Insulator at the Ultrathin Limit: MgO on Ag(001). *Phys. Rev. Lett.* **2001**, *87*, 276801.
15. Klaua, M.; Ullmann, D.; Barthel, J.; Wulfhekel, W.; Kirschner, J.; Urban, R.; Monchesky, T. L.; Enders, A.; Cochran, J. F.; Heinrich, B. Growth, Structure, Electronic, and Magnetic Properties of MgO/Fe(001) Bilayers and Fe/MgO/Fe(001) Trilayers. *Phys. Rev. B* **2001**, *64*, 134411.
16. Valeri, S.; Altieri, S.; del Pennino, U.; di Bona, A.; Luches, P.; Rota, A. Scanning Tunnelling Microscopy of MgO Ultrathin Films on Ag(001). *Phys. Rev. B* **2002**, *65*, 245410.
17. Schintke, S.; Schneider, W.-D. Insulators at the Ultrathin Limit: Electronic Structure Studied by Scanning Tunnelling Microscopy and Scanning Tunnelling Spectroscopy. *J. Phys.: Condens. Matter* **2004**, *16*, R49.
18. Barth, C.; Henry, C. R. Atomic Resolution Imaging of the (001) Surface of UHV Cleaved MgO by Dynamic Scanning Force Microscopy. *Phys. Rev. Lett.* **2003**, *91*, 196102.
19. Heyde, M.; Sterrer, M.; Rust, H.-P.; Freund, H.-J. Atomic Resolution on MgO(001) by Atomic Force Microscopy Using a Double Quartz Tuning Fork Sensor at Low-Temperature and Ultrahigh Vacuum. *Appl. Phys. Lett.* **2005**, *87*, 083104.
20. König, T.; Simon, G. H.; Rust, H.-P.; Pacchioni, G.; Heyde, M.; Freund, H.-J. Measuring the Charge State of Point Defects on MgO/Ag(001). *J. Am. Chem. Soc.* **2009**, *131*, 17544–17545.
21. König, T.; Simon, G. H.; Rust, H.-P.; Heyde, M. Work Function Measurements of Thin Oxide Films on Metals—MgO on Ag(001). *J. Phys. Chem. C* **2009**, *113*, 11301–11305.
22. Olbrich, A.; Ebersberger, B.; Boit, C.; Vancea, J.; Hoffmann, H.; Altmann, H.; Gieres, G.; Wecker, J. Oxide Thickness Mapping of Ultrathin $Al_2O_3$ at Nanometer Scale with Conducting Atomic Force Microscopy. *Appl. Phys. Lett.* **2001**, *78*, 2934–2936.
23. Steurer, W.; Surnev, S.; Fortunelli, A.; Netzer, F. P. Scanning Tunneling Microscopy Imaging of NiO(100)(1 × 1) Islands Embedded in Ag(100). *Surf. Sci.* **2012**, *606*, 803–807.
24. Giessibl, F. J. Atomic Resolution on Si(111)-(7 × 7) by Noncontact Atomic Force Microscopy with a Force Sensor Based on a Quartz Tuning Fork. *Appl. Phys. Lett.* **2000**, *76*, 1470–1472.
25. Sgroi, M.; Pisani, C.; Busso, M. *Ab Initio* Density Functional Simulation of Structural and Electronic Properties of MgO Ultra-thin Adlayers on the (001) Ag Surface. *Thin Solid Films* **2001**, *400*, 64–70.
26. Albrecht, T. R.; Grütter, P.; Horne, D.; Rugar, D. Frequency Modulation Detection Using High-*Q* Cantilevers for Enhanced Force Microscope Sensitivity. *J. Appl. Phys.* **1991**, *69*, 668–673.
27. Ternes, M.; Lutz, C. P.; Hirjibehedin, C. F.; Giessibl, F. J.; Heinrich, A. J. The Force Needed To Move an Atom on a Surface. *Science* **2008**, *319*, 1066–1069.
28. Heinrich, V. E.; Cox, P. A. *The Surface Science of Metal Oxides*; Cambridge University Press: New York, 1994.
29. Kiguchi, M.; Goto, T.; Saiki, K.; Sasaki, T.; Iwasawa, Y.; Koma, A. Atomic and Electronic Structures of MgO/Ag(001) Heterointerface. *Surf. Sci.* **2002**, *512*, 97–106.
30. Ferrari, A. M.; Casassa, S.; Pisani, C. Electronic Structure and Morphology of MgO Submonolayers at the Ag(001) Surface: An *Ab Initio* Model Study. *Phys. Rev. B* **2005**, *71*, 155404.
31. Hebenstreit, W.; Redinger, J.; Horozova, Z.; Schmid, M.; Podloucky, R.; Varga, P. Atomic Resolution by STM on Ultra-thin Films of Alkali Halides: Experiment and Local Density Calculations. *Surf. Sci.* **1999**, *424*, L321–L328.
32. Wintterlin, J.; Bocquet, M.-L. Graphene on Metal Surfaces. *Surf. Sci.* **2009**, *603*, 1841–1852. Special Issue of Surface Science dedicated to Prof. Dr. Dr. h.c. mult. Gerhard Ertl, Nobel-Laureate in Chemistry 2007.
33. Repp, J.; Meyer, G. Scanning Tunneling Microscopy of Adsorbates on Insulating Films. From the Imaging of Individual Molecular Orbitals to the Manipulation of the Charge State. *Appl. Phys. A: Mater. Sci. Process.* **2006**, *85*, 399–406.
34. Altieri, S.; Tjeng, L. H.; Sawatzky, G. A. Electronic Structure and Chemical Reactivity of Oxide−Metal Interfaces: MgO-(100)/Ag(100). *Phys. Rev. B* **2000**, *61*, 16948–16955.
35. Sterrer, M.; Heyde, M.; Novicki, M.; Nilius, N.; Risse, T.; Rust, H.-P.; Pacchioni, G.; Freund, H.-J. Identification of Color Centers on MgO(001) Thin Films with Scanning Tunneling Microscopy. *J. Phys. Chem. B* **2006**, *110*, 46–49.